Enhanced cell survival and therapeutic benefits of IL-10-expressing multipotent mesenchymal stromal cells for muscular dystrophy

Yuko Nitahara-Kasahara[1,2,3*], Mutsuki Kuraoka[3,4], Yuki Oda[1], Hiromi Hayashita-Kinoh[1,2,3], Shin'ichi Takeda[3] and Takashi Okada[1,2,5*]

[1]Department of Biochemistry and Molecular Biology, Nippon Medical School, Bunkyo-city, Tokyo, Japan

[2]Division of Cell and Gene Therapy, Nippon Medical School, Bunkyo-city, Tokyo, Japan

[3]Department of Molecular Therapy, National Institute of Neuroscience, National Center of Neurology and Psychiatry, Kodaira, Tokyo, Japan

[4]Laboratory of Experimental Animal Science, Nippon Veterinary and Life Science University, Musashino, Tokyo, Japan

[5]Division of Molecular and Medical Genetics, Center for Gene and Cell Therapy, Institute of Medical Science, University of Tokyo, Tokyo, Japan

[*]Correspondence should be addressed to Takashi Okada, M.D, PhD
Division of Molecular and Medical Genetics, Center for Gene and Cell Therapy,
Institute of Medical Science, University of Tokyo,
4-6-1 Shirokanedai, Minato-ku, Tokyo 108-8639, Japan
Telephone:+81-3-5449-5528
E-mail: t-okada@ims.u-tokyo.ac.jp

[*]Co-correspondence should be addressed to: Yuko Nitahara-Kasahara, PhD
Department of Biochemistry and Molecular Biology, Nippon Medical School,
1-1-5 Sendagi, Bunkyo-city, Tokyo, Japan
Telephone: +81-3-3822-2131

E-mail: y-kasahara@nms.ac.jp

Abstract

Background:

Multipotent mesenchymal stromal cells (MSCs) are potentially therapeutic for muscle disease because they can accumulate at the sites of injury and are immunosuppressive. MSCs are attractive candidates for cell-based strategies that target diseases with chronic inflammation, such as Duchenne muscular disease (DMD). We focused on the IL-10 based on anti-inflammatory properties and hypothesized that IL-10 could increase the typically low survival of MSCs by exerting a paracrine effect after transplantation.

Methods:

We developed a continuous IL-10 expression system of MSCs using an adeno-associated virus (AAV) vector. To investigate the potential benefits of using AAV/IL-10 vector-transduced MSCs (IL-10-MSCs), we examined the cell survival rates in the skeletal muscles after intramuscular injection into mice and dogs. The systemic treatment of IL-10-MSCs derived from dental pulp (DPSCs) was comprehensive analyzed using the canine X-linked muscular dystrophy model in Japan ($CXMD_J$), which has a severe phenotype similar to DMD patient.

Results:

In vivo bioluminescence imaging analysis revealed higher retention of IL-10-MSCs injected into the hind-limb muscle of mice. In the muscles of dogs, myofiber-like tissue was formed after the stable engraftment of IL-10-MSCs. Repeated systemic administration of IL-10-DPSCs into $CXMD_J$ model resulted in long-term engraftment of cells, slightly increased serum levels of IL-10. IL-10-hDPSCs showed remarkably

reduced the expression of pro-inflammatory MCP-1 and IL-6, and upregulated stromal-derived factor-1 (SDF-1). In fact, MRI and histopathology of the hDPSC-treated $CXMD_J$ indicated the regulation of inflammation in the muscles, but not myogenic differentiation from treated cells. hDPSC-treated $CXMD_J$ showed improved running capability, and recovery in tetanic force with concomitant increase in physical activity. Serum creatine kinase levels, which increased immediately after exercise, were suppressed in the IL-10-hDPSC-treated $CXMD_J$.

Conclusions:

In case of local injection, IL-10-MSCs could maintain the long-term engraftment status and facilitate associated tissue repair. In case of repeated systemic administration, IL-10-MSCs facilitated the long-term retention of the cells in the skeletal muscle and also protected muscles with physical damage-induced injury, which improved muscle dysfunction in DMD. We can conclude that the local and systemic administration of IL-10-producing MSCs offers potential benefits for DMD therapy, through the beneficial IL-10 paracrine effects and may exert SDF-1.

Keywords: Mesenchymal stromal cells, IL-10, DMD

Background

Multipotent mesenchymal stromal cells (MSCs) derived from the bone marrow are conventionally termed adherent non-hematopoietic cells. The cells express several cell-surface antigenic markers, including CD44, CD73, CD90, and CD105 [1]. MSCs can self-renew and differentiate into several different cell types. These include cells of mesodermal origin, such as osteoblasts, chondrocytes, adipocytes, and myocytes [2-4], as well as cells of non-mesodermal origin, such as hepatocytes [5], neural cells [6], and epithelial cells [7].

The multi-lineage potential of MSCs has been exploited for prospective use in therapies for various diseases. The cells can be easily expanded in culture and are non-tumorigenic. Furthermore, the use of MSCs as third-party materials in cell therapy reflects that MSCs are immune-privileged, unlike other stem cells or induced pluripotent stem cells (iPS), as they do not express human leukocyte antigen (HLA) class II, CD40, CD80, or CD86 molecules [8], and express only low levels of HLA class I. These cells are not lysed by natural killer cells or cytotoxic T lymphocytes [9]. MSCs can influence immune effector cell development, maturation, and function as well as reactive T-cell responses through the production of bioactive cytokines and proteins [10, 11]. The mechanism underlying the immunosuppressive effects of MSCs are unclear. Nonetheless, their immunosuppressive properties have been exploited in clinical applications. MSCs are commercially authorized for the treatment of acute graft-versus-host disease (GVHD). MSCs are attractive candidates for cell-based strategies that target diseases with chronic inflammation, such as Duchenne muscular dystrophy (DMD) [11].

Interleukin-10 (IL-10) is an anti-inflammatory cytokine with anti-apoptotic properties [12] that modulates the inflammatory immune response. IL-10 reduces M1

91 macrophage activation and inhibits the production of pro-inflammatory cytokines such as
92 interferon-gamma (IFN-γ), tumor necrosis factor-alpha (TNF-α), IL-1β, and IL-6 in
93 inflamed tissues [13, 14]. IL-10 also reduces the expression of CD54, CD80, CD86, and
94 major histocompatibility complex class II molecules, resulting in incomplete T-cell
95 signaling and the induction of antigen-specific anergy. We hypothesized that IL-10 could
96 increase the typically low survival of MSCs by exerting a paracrine effect after
97 transplantation. IL-10-expressing MSCs were previously developed using retroviral [15,
98 16], lentiviral vectors [17], and transcription activator-like effector nuclease (TALENs)-
99 mediated gene editing [18]. They have therapeutic benefits in collagen-induced
100 inflammatory arthritis [19], besides preventing lung ischemia-reperfusion injury [15],
101 GVHD [16], traumatic brain injury [17], and left ventricular remodeling after myocardial
102 infarction [18].

103 We developed a continuous IL-10 expression system of MSCs using an adeno-
104 associated virus (AAV) vector. AAV vectors are safe and do not integrate into the host
105 cell genome, and the risk of insertional mutagenesis is low. To investigate the potential
106 benefits of using MSCs for treating muscle disease, we examined whether the MSCs
107 transduced with the IL-10-expressing AAV vector enhances the survival rates of
108 themselves in skeletal muscles, and the potential advantages offered by MSC
109 transplantation. The systemic treatment using MSCs derived from dental pulp (dental
110 pulp stem cells, DPSCs) was comprehensive analyzed using the canine X-linked
111 muscular dystrophy model in Japan ($CXMD_J$), which has a severe phenotype similar to
112 DMD in humans [20, 21]. DPSCs are similar to bone marrow MSCs, which showed high
113 expression of the surface markers CD29, CD73, CD90, and CD105, as common stem cell
114 markers in MSCs, but not CD34 or CD45. We previously reported DPSCs also highly

expressed IL-10 and vascular endothelial growth factor (VEGF) and immunosuppressive activities [22, 23]. We evaluated whether DPSCs expressing IL-10 play an important role as a cell source for DMD therapy.

Materials and Methods

Animals

NOD/SCID mice were purchased from Nihon CLEA (Tokyo, Japan) and were housed at the National Center of Neurology and Psychiatry (Tokyo, Japan). All experiments using mice were performed in accordance with the guidelines approved by the Nippon Medical School and National Center of Neurology and Psychiatry (NCNP) Animal Ethics Committees. Beagle dogs and $CXMD_J$ colony dogs were maintained according to the NCNP standard protocol for animal care. Experiments were performed in accordance with the guidelines approved by the Ethics Committee for the Treatment of Laboratory Animals at NCNP.

Cell preparation

MSCs derived from rat bone marrow were isolated and expanded as previously described [24]. For the experiments on dogs, healthy donor dogs were anesthetized using thiopental and isoflurane, and 1.0 mL of bone marrow fluid was collected. The $CD271^+$ MSCs were enriched and cultivated using the MSC Research Tool Box-CD271 (LNGFR) containing CD271 (LNGFR)-PE and Anti-PE Micro Beads for cell separation (Miltenyi Biotec GmbH, Bergisch Gladbach, Germany), as previously reported [25]. Human DPSCs were provided by JCR Pharmaceuticals (Hyogo, Japan). The cells were cultured in Dulbecco's modified Eagle's medium (DMEM, Thermo Fisher Scientific, Waltham, MA)

supplemented with 10% fetal bovine serum (FBS, Thermo Fisher Scientific) and 1% antibiotic-antimycotic solution (FUJIFILM Wako Pure Chemical Industries, Osaka, Japan) at 37°C in a 5% CO_2 atmosphere.

Cell culture and gene transduction

To generate luciferase-expressing MSCs, the MSCs isolated from Sprague-Dawley rat bone-marrow[24] were transduced with vesicular stomatitis virus-glycoprotein (VSV-G)-pseudotyped retroviral vector encoding firefly luciferase [26]. Canine $CD271^+$ MSCs were transduced with a luciferase-expressing retroviral vector, followed by transduction with enhanced green fluorescent protein (eGFP) or MyoD-expressing adenoviral vector (Ad C2-eGFP or Ad C2-MyoD), as we previously reported [25]. To assess the long-term effects of IL-10 expression, MSCs or DPSCs were transduced with AAV1/eGFP or control AAV1/IL-10 vectors developed according to methods described previously [27, 28]. All the cells were maintained in DMEM supplemented with 10% FBS as well as 100 U/mL penicillin and 100 μg/mL streptomycin (Sigma-Aldrich, St. Louis, MO). For preparation of transplantation, cells were washed with PBS to remove the culture medium containing vectors, completely.

Transplantation of MSCs into mice

Luciferase-expressing MSCs (Luc-MSCs, 5.0−10.0 × 10^6 cells) were injected intramuscularly into the right- or left side hind-limb muscle of NOD/SCID mice. AAV1/IL-10- or eGFP-vector-transduced Luc-MSCs (1.0 × 10^7 cells, Figure 1) were intramuscularly injected into the right side (eGFP-MSCs) and the left side (IL-10-MSCs) hind-limb muscle of NOD/SCID mice.

In vivo imaging analysis

After the injection of Luc-MSCs on day 0 of the experiment, *in vivo* luminescence images were acquired periodically to assess the engraftment efficiency and cell survival in the transplanted mice. Prior to imaging, the mice were anesthetized by inhalation of 2.0% isofluorane and oxygen and injected intraperitoneally with 150 mg luciferin (Summit Pharmaceuticals International Corp., Tokyo, Japan.) per kg body weight. *In vivo* images were acquired using the IVIS charge-coupled-device camera system (Xenogen Corp., Alameda, CA) at multiple time points (0, 3, 7, 18, 27, 31, 34, 42, 49, 54, and 67 days after transplantation). The region of interest (ROI) luminescence signals from individual MSC-injected sites were calculated using the Living Image® 3.2 software package (Xenogen Corp.).

Transplantation into dogs

IL-10-transduced Luc-CD271$^+$ MSCs (2.4–2.7 × 10^7 cells/2 mL) were injected into the muscles of healthy Beagle dogs. Five days before the treatment, muscle degeneration and regeneration cycles were induced in the tibialis anterior (TA) muscles by injecting 10 nmol/kg cardiotoxin (C9759, Sigma-Aldrich, St. Louis, MO) under the maintenance of anesthesia. For analgesia treatment, 0.02 mg/kg of buprenorphine hydrochloride (Lepetan, Otsuka Pharmaceutical, Tokyo, Japan) was injected intramuscularly before the dogs awoke from general anesthesia. On day 0 and day 50 of the experiment, MSCs were injected into pretreated muscles without using immunosuppressants. The injected muscles were then biopsied at 4 weeks after the treatment, or the animals were sacrificed at 8 weeks after transplantation. The dogs underwent periodic veterinary examinations

during the experiments.

hDPSCs or IL-10-transduced hDPSCs (4.0×10^6 cells/mL/kg body weight at a rate of 1 mL/min) were given via intravenous injection into $CXMD_J$ that were pretreated with polaramine (chlorpheniramine maleate, 0.15 mg/kg, MSD) by nine injections at 2-week intervals (Table I). After each injection, the activity, heart rate, respiratory rate, and signs of abnormalities were carefully monitored. Weight measurement and blood tests were performed weekly to examine the side effects of repeated cell treatment.

For biopsy and necropsy, the individual muscles were sampled for tendon-to-tendon dissection, divided into several fragments, and immediately frozen in liquid nitrogen-cooled isopentane for histological analysis. Whole muscle tissue homogenates were prepared using a POLYTRON homogenizer (150–180 min^{-1}) and Multi-Beads Shocker (Yasui Kikai Corp. Osaka, Japan).

Blood test

The dogs underwent periodic veterinary examinations at 1−2 week intervals until sampling. Hematological and serum biochemical testing for CK was performed using a model F-820 semi-automated hematology analyzer (Sysmex, Hyogo, Japan). The levels of serum ALT, alkaline phosphatase, aspartate aminotransferase (AST) and blood urea nitrogen (BUN) were determined using a DRI-CHEM3506 automated analyzer (Fuji Film, Tokyo, Japan).

Histopathological and immunohistochemical analyses

Samples from MSC-treated TA muscles were collected and immediately frozen in liquid nitrogen-cooled isopentane. Five mice from each group were used for analysis at each

time point. Transverse cryosections 8μm in thickness prepared from the skeletal muscles were stained with H&E using standard procedures. For immunohistochemical analyses, thick cryosections were fixed in acetone for 5 min at –20°C. The tissue sections were then blocked with 0.5% bovine serum albumin (BSA) in PBS. The following antibodies were used for antigen detection at 1:40–1:50 dilutions: rabbit anti-firefly luciferase (ab21176; Abcam Plc., Cambridge, UK) and mouse anti-dystrophin (NCL-DYS3, Leica, Wetzlar, Germany). These antibodies were diluted using 0.5% BSA in PBS and incubated with the cells or tissue sections overnight at 4°C. The tissue sections were washed with PBS and then probed with Alexa 568-conjugated anti-rabbit IgG antibodies (Thermo Fisher Scientific) and Alexa 488-conjugated anti-mouse IgG antibodies (Thermo Fisher Scientific) at 1:250–1:100 dilution for 1 h at 4°C. The coverslips slides were washed with PBS and mounted in Vectashield (Vector Laboratories Inc., Burlingame, CA) with 4′,6′ -diamidino-2-phenylindole (DAPI). Immunofluorescence was performed using an IX71 fluorescence microscope (Olympus, Tokyo, Japan).

To confirm the presence of transplanted cells at the injection sites, the MSCs were labeled with luciferase or eGFP. The tissue sections were incubated in a solution of 3% H_2O_2 to block endogenous peroxidase. The nonspecific binding sites were blocked with 2% BSA solution. The tissue sections were probed with primary antibodies for 1 h and then treated using the 3,3'-diaminobenzidine (DAB) substrate kit (Vector Laboratories Inc.) containing horseradish peroxidase (HRP) as an enzyme indicator. The slices were then subjected to DAB chromogen staining to determine the form of the brown-antigen reaction product. The tissue sections were visualized using an IX71 microscope (Olympus).

ELISA

IL-10 expression levels were measured in the FBS-free MSC culture medium after 2 days of incubation, in the TA muscle lysate, and in the serum obtained from animals using the Quantikine ELISA mouse or canine IL-10 immunoassay (Thermo Fisher Scientific) and canine IL-6 and INF-γ immunoassay (R&D Systems, Inc., Minneapolis, MN) according to the manufacturer's recommendations. The final values were normalized to the protein concentrations, which were determined using the Pierce® BCA Protein Assay Kit (Thermo Fisher Scientific).

Luciferase reporter assays

Luciferase reporter assays were performed to evaluate the retention of Luc-MSCs in the TA muscle. Firefly luciferase activity was tested in whole tissue homogenates using the Bright-Glo™ Luciferase Assay System (Promega Corporation, Madison, WI) according to the manufacturer's instructions. Luciferase levels were measured on a Varioskan LUX Multimode Microplate Reader (Thermo Fisher Scientific). Protein concentrations were measured using a Pierce® BCA Protein Assay Kit (Thermo Scientific Pierce, Rockford, IL). The experiments were performed in duplicates in three independent experiments.

Biodistribution of MSCs

The tissue samples were disrupted in a Multi-Beads Shocker (Yasui Kikai Co., Ltd., Osaka, Japan). DNA was extracted from tissue suspensions using a DNeasy Blood and Tissue kit (QIAGEN, Valencia, CA) and quantified with a NanoDrop spectrophotometer (Thermos Fisher Scientific). Real-time qPCR was performed using 125 ng of DNA in a total volume of containing DNA Master SYBR Green I kit (Roche Diagnostics, Basel,

Switzerland) and primers for *Alu* or murine *glyceraldehyde 3-phosphae dehydrogenase* (*Gapdh*). The primer sequences used were as follows: human *Alu*, 5′-GTCAGGAGATCGAGACCATCCC-3′ (forward) and 5′-TCCTGCCTCAGCCTCCCAAG-3′ (reverse); for murine *Gapdh*, 5′-GATGACATCAAGAAGGTGGTGA-3′ (forward) and 5′-TGCTGTAGCCGTATTCATTGTC-3′ (reverse). PCR conditions were as follows: 95°C for 2 min, followed by 40 cycles at 95°C for 15 s and 68°C for 30 s, and at 72°C for 30 s. The standard was generated by adding 10-fold serial dilutions of human DPSCs to determine the number of human DPSCs in 125 ng of DNA that was used in the PCR reaction for each organ sample. We extrapolated the quantity of DNA isolated from each organ to determine the number of human DPSCs per organ.

Real-time PCR

Total RNA (1 μg) was isolated from muscle samples disrupted in a Multi-Beads Shocker (Yasui Kikai Co., Ltd.) using the RNeasy Micro kit (QIAGEN). First-strand complementary DNA was synthesized using a Super Script III First-Strand Synthesis System for reverse transcriptase-PCR (Invitrogen, Carlsbad, CA). From 20 μL of the complementary DNA reaction volume, 0.5 to 2 μL was used for each PCR assay using mouse *Il6* and *Gapdh* as an internal control. The primer sequences used were as follows: 5′-AGTGTTCTCAAGGTCCGAGTCC-3′ (forward) and 5′-AAATCTCTGGACAGGCTTCAGG-3′ (reverse). PCR conditions were as follows: 95°C for 2 min, followed by 40 cycles at 95°C for 15 s and 68°C for 30 s, and at 72°C for 30 s. Quantitative PCR was performed by SYBR green detection in PCR products in real-time

using the MyiQ single-color detection system (Bio-Rad, Hercules, CA).

Proteome cytokine/cytokine array

The FBS-free DPSC culture medium was collected after 2 days of incubation for array analysis. The relative expression of cytokines and chemokines in the culture medium was quantified using the Proteome Profiler™ Array (Mouse Cytokine Array, Panel A; R&D Systems Inc.), as previously described [26]. To achieve maximum assay sensitivity, the blots were incubated overnight with plasma. Enhanced chemiluminescence incubation was performed for 5 min using the Super Signal West Femto Chemiluminescence Kit (Thermo Scientific Pierce), and the samples were imaged and analyzed using the Image Quant LAS 4000 coupled with Image Quant TL software (GE Healthcare Japan, Tokyo, Japan) and Image J software (NIH, Bethesda, MD).

Locomotor activity analyses

Physical activity levels of CXMD$_J$ and littermate normal dogs used as controls were monitored during the experimental period using an infrared sensor system (Supermex, Muromachi Kikai Co., Ltd., Tokyo, Japan) as previously described [29]. These systems monitor and enumerate all spontaneous movements. The average of all counts of spontaneous locomotor activity in animals determined over 5 days and nights (12 h light/dark cycles) was calculated. Further, we measured the 15-m running time of normal and CXMD$_J$ littermates during the experimental period. The running speed was averaged four times.

Magnetic resonance imaging (MRI)

$CXMD_J$ anesthetized by injection (20 mg/kg) were intubated using an endotracheal tube, and general anesthetization was maintained using an inhalational mixture of 2 to 3% isofluorane and oxygen. Heart rate and oxygen saturation were monitored continuously. Images of the T2-weighted and fat-saturated T2-weighted series were captured using the same method as described in a previous study [30]. We examined the crus muscles of the lower limbs using a superconducting 3.0-Tesla MRI device (MAGNETOM Trio; Siemens Medical Solutions, Erlanger, Germany) with an 18-cm diameter/18-cm length human extremity coil. The images were analyzed quantitatively using the Syngo MR2004A software (Siemens Medical Solutions), as previously reported [30, 31]. Briefly, the ROIs were selected to avoid flow artifacts and large vessels and the signal intensities were measured for these ROIs. The SNRs for each ROI were calculated using the following equation: SNR = signal intensity/SDair, where SDair is the standard deviation (SD) of the background noise. The average SNR (Ave SNR) was calculated using the equation described in our previous report [31]. The analysis was performed on the right and left side TA muscle, EDL, gastrocnemius medial head, GL, flexor digitorum superficialis, flexor digitorum longus, and flexor hallucis longus muscle.

Hind-limb extensor strength test

The functional status of the two hind limbs in the $CXMD_J$ was evaluated by measuring the flexion and extension strengths of the wrist using a customized torque measurement device. Stimulation frequencies from 60 Hz can activate muscles that extend or push the hind paw against the ground. A transducer captures the torque generated when the paw

pushes against the force plate. The maximal torque was expressed as a percentage of predicted values computed using a model based on control values with respect to the animal weight. $P< 0.05$ was considered statistically significant [32].

Statistical analyses

Data are presented as mean ± SD. Differences between the two groups were assessed using unpaired two-tailed *t*-tests. Multiple comparisons between three or more groups were performed using one-way or two-way ANOVA. Statistical significance was defined by $^{*}P < 0.05$, $^{**}P < 0.01$, $^{***}P < 0.001$, and $^{****}P < 0.0001$, and was calculated using Excel (Microsoft, Redmond, WA) and GraphPad Prism 8 (GraphPad, La Jolla, CA).

Results

Enhanced engraftment of IL-10-expressing MSCs

In vivo bioluminescence imaging analysis revealed a 1.7-fold higher retention of IL-10-expressing MSCs injected into the hind-limb muscle of NOD/SCID mice compared to the retention of MSCs alone 4 days after injection (*Figures S1A, B*). When luciferase (Luc)-MSCs were injected together AAV1/IL-10 or AAV/Lac Z control vector, which were not transduced into the cells, there was no significant difference in cell survival of the Luc-MSCs-treated mice (*Figures S1C, D*). IL-10 plasmid-transfected Luc-MSCs expressed higher levels of IL-10 and were more effective at enhancing post-transplantation retention. We also confirmed a maximum 69-fold stronger signal intensity of luciferase in muscles transplanted with IL-10-expressing MSCs compared to the control MSC-treated muscles at day 7 (*See also Figure S2*), although these cells were disappeared within the few days. We developed a continuous IL-10 expression system of

MSCs using an AAV vector to verify the expected high and prolonged cell survival rates following transplantation. Significantly higher levels of IL-10 expression from AAV1/IL-10-transduced Luc-MSCs (IL-10-Luc-MSCs) were confirmed *in vitro* (Figure 1A) and in treated muscles (*See also Figure S3*). Conversely, downregulation of pro-inflammatory IL-6 was evident compared with that in AAV1/ eGFP-transduced Luc-MSCs (GFP-Luc-MSCs, $p < 0.0001$, Figure 1B). IL-10-Luc-MSCs displayed a higher cell survival rate immediately after administration (luciferase signal at 3 days after transplantation, $4.41 \pm 1.78 \times 10^5$ counts) with a maximum of 6.5-fold at 24 days ($3.46 \pm 1.12 \times 10^4$ counts) compared to the signal of GFP-Luc-MSCs ($2.98 \pm 1.04 \times 10^5$ counts, $p < 0.0001$; $5.35 \pm 2.93 \times 10^3$ counts, $p = 0.002$, respectively), as observed *in vivo* in imaging analysis (Figure 1C, *D*; *See also Figure S4*). The findings suggested that the higher retention in the early stage had a significant effect on long-term engraftment. Notably, retention of IL-10-Luc-MSCs was more than 67 days after transplantation (Figure 1C; IL-10-Luc-MSCs, 78.6 ± 65.2 pg/mL).

Successful long-term engraftment of IL-10-MSCs in injured muscle tissue

We also investigated the effects of IL-10 overexpression using Beagle dogs as a larger animal model (Figure 2A, Table I). $CD271^+$MSCs transduced with an AAV1-IL-10 (IL-10-Luc-$CD271^+$MSCs) showed overexpression of IL-10 in the culture medium (MyoD-MSCs, 3.1 pg/mL; IL-10-MSCs, 93.6 pg/mL). Four weeks after intramuscular injection, accumulation of IL-10-Luc-$CD271^+$MSCs was observed in immunochemical analysis of the cardiotoxin-injured tibialis anterior (TA) muscle (Figure 2B). In addition, immunofluorescence analysis revealed the accumulation of luciferase-positive IL-10-Luc-$CD271^+$MSCs around the inflammatory region in MSC-treated TA muscle 4 weeks

after the secondary injection (Figure 2C). Luciferase-positive muscle-like tissue was detected in the IL-10-Luc-CD271$^+$MSC-treated muscle, similar to that observed in the muscle after treatment with Luc-CD271$^+$ MSCs transduced with MyoD (MyoD-Luc-CD271$^+$MSC), which is a key factor for myogenic determination, as described in our previously report [25]. These findings suggest that the Luc-CD271$^+$MSCs transduced with AAV1/IL-10 formed myofibers even in absence of myogenic stimulation. Luciferase activity, which was correlated to the number of MSCs, was twice as high in IL-10-Luc-CD271$^+$MSC-treated TA muscle compared to that in MyoD-Luc-CD271$^+$MSC-treated muscle (Figure 2D). The IL-10 levels in IL-10-Luc-CD271$^+$MSC-treated TA muscles increased, while those in MyoD- Luc-CD271$^+$MSC-treated muscles did not (Figure 2E). These data suggest that more IL-10-expressing CD271$^+$MSCs could survive and engraftment could be maintained after intramuscular injection during muscle regeneration.

Safety and efficacy of systemic transplantation of IL-10-DPSCs in the DMD model

Next, we evaluated the efficacy of IL-10-expressing MSCs by systemic transplantation using hDPSCs (Figure 3A). We confirmed that extracellular secretion of IL-10 from AAV1/IL-10-transduced-human DPSCs (IL-10-hDPSCs) remarkably reduced the expression of pro-inflammatory monocyte chemotactic protein-1 (MCP-1) and IL-6, and conversely upregulated stromal-derived factor-1 (SDF-1) in IL-10-hDPSCs compared with the levels in hDPSCs (Figures 3B, C). IL-10-hDPSCs or hDPSCs were intravenously injected nine times at biweekly intervals in the acute phase in the CXMD$_J$ model with the DMD phenotype (Table I). No obvious abnormalities related to liver damage, kidney damage, or anemia were induced in response to the systemic administration in the hDPSC-treated CXMD$_J$. Transient increases in ALT, AST, and BUN levels was observed

occasionally in the CXMD$_J$ model, independent of treatment with hDPSCs (*See also Figure S5*). During the experiment, the IL-10-hDPSC-treated CXMD$_J$ showed better growth compared to the untreated littermates, CXMD$_J$ ($p < 0.0001$), and the hDPSC-treated CXMD$_J$ ($p < 0.0001$) in terms of body weight (Figure 3D) and larger femur circumference (*See also Figure S6*). Although the serum levels of IL-10 were increased transiently 6 h after IL-10-hDPSC injection (104.0 pg/mL vs. control DMD, vs. hDPSC-DMD, $p < 0.0001$), the levels reduced rapidly within 24 h of transplantation (32.6 pg/mL vs. control DMD, $p < 0.0067$; vs. hDPSC-DMD, $p < 0.0278$), and did not differ significantly from the control CXMD$_J$ 7 days after injection (21.6 pg/mL) (Figure 3E). Cell retention in blood was similar to that of hDPSCs (1.79e-04 ± 1.95e-04 ng/100 ng genomic DNA) and IL-10-hDPSCs 24 h after transplantation (7.94e-04 ± 7.89e-05 ng/100 ng genomic DNA), as revealed by human-specific *Alu*-PCR. The long-term engraftment in tissue was investigated. No hDPSCs were detected in the skeletal muscle, lung, or liver tissues of the hDPSC-treated CXMD$_J$. IL-10-hDPSCs could only survive and maintain the engraftment status in the TA muscle (56.1 pg/100 ng genomic DNA) 4 months after treatment, and were not detected in other organs.

Morphological improvement in IL-10-hDPSC-treated DMD dog

The high-intensity T2-signals in MRI, which were detected in the necrotic/edematous and inflammatory lesions in the dystrophic muscle, were significantly reduced in the cross-sectional muscles of the IL-10-hDPSC-treated dog (82.5 ± 16.9 average signal-to-noise ratios, SNRs) compared to the signals in hDPSC-treated CXMD$_J$ (97.4 ± 13.3, $p = 0.008$) after transplantation (Figure. 4A, B). The gastrocnemius lateral (GL) and extensor digitorum longus (EDL) muscles from CXMD$_J$ displayed signs of immune cell

infiltration and degenerating myofibers (Figure 4C). In contrast, the histopathological observations of the hDPSC- and IL-10-hDPSC-treated $CXMD_J$ muscles revealed significantly limited infiltration of nuclei, which indicated a milder phenotype compared to untreated $CXMD_J$. The levels of IL-6 in blood increased transiently in $CXMD_J$ (maximum 742.9 pg/mL). In contrast, the levels in IL-10-hDPSC-treated $CXMD_J$ were within the normal range (0–9.85 pg/mL), during the experiments. High levels of IFN-γ were also observed in $CXMD_J$ (maximum 103.9 pg/mL) and hDPSC-treated $CXMD_J$ (114.8 pg/mL), whereas they tended to be marginally lower in the IL-10-hDPSC-treated $CXMD_J$ (68.4 pg/mL) compared to that in other groups. These data suggest that the repeated systemic administration of IL-10-hDPSCs produces morphological improvement, including regulated inflammation in $CXMD_J$.

Long-term maintenance of muscle function in IL-10-hDPSC-treated DMD dog

$CXMD_J$ developed progressive general weakness owing to the reduced strength in the skeletal muscles. The tetanic force on hind limbs in $CXMD_J$ (2.55 ± 0.42 N·m/s) was 41.2 ± 5.1% of that in normal dogs ($p < 0.0001$) in *Figure S7*. Conversely, significantly stronger torque values were observed in the IL-10-hDPSC-treated $CXMD_J$ (4.17 ± 1.28 N·m/s, 66.5 ± 12.2% of the value in the normal dog, $p < 0.0001$) than in $CXMD_J$ ($p < 0.0008$), similar to that in the hDPSC-treated $CXMD_J$ (3.68 ± 0.57 N·m/s). These results suggest that the progressive loss of limb muscle strength is ameliorated upon treatment with hDPSCs and IL-10-hDPSCs.

Additionally, the physical activity of $CXMD_J$ in the home cage also underwent a dramatic reduction with age compared to that in normal dogs (Figure 5A) [29]. Improved the activity was confirmed in both groups, the hDPSC-treated (8340.4 ± 1090.3

444 counts; vs. control DMD, p = 0.0006) and IL-10-hDPSC-treated CXMD$_J$ (8531.6 ±
445 1146.5 counts; vs. control DMD, $p < 0.0001$), which was observed upon the comparison
446 of one-year-old CXMD$_J$ littermates with advanced symptoms (3954.4 ± 792.0 counts)
447 (Figure 5A). The IL-10-hDPSC-treated CXMD$_J$ exhibited persistent and predominantly
448 higher activity (6 months; 13008.8 ± 1367.1 counts) than CXMD$_J$ (9926.0 ± 1436.8
449 counts, p = 0.0268) as well as hDPSC-treated CXMD$_J$ (12605.8 ± 1756.3 counts).
450 Furthermore, hDPSC- or IL-10-hDPSC-treated CXMD$_J$ maintained their 15-m running
451 speed, and were active at 3 to 12 months of age (Figure 5B, *see also Figure S8, and Table*
452 *S1*; normal *vs.* control DMD, $p < 0.0001-0.0062$; control DMD *vs*. hDPSC-DMD, p =
453 0.0025−0.0104; control DMD *vs*. IL-10-hDPSC-DMD, p = 0.0012−0.0113). There was
454 no significant difference in the running speed between hDPSC-, and IL-10-hDPSC-
455 treated CXMD$_J$. However, the increased serum creatine kinase (CK) levels after running
456 exercise (50595 ± 67255 unit/L) were recovered immediately until 20 min in IL-10-
457 hDPSC-treated CXMD$_J$ (Figure 5C, 16490 ± 4850 unit/L; *vs.* hDPSC-treated DMD, p =
458 0.0134). Conversely, a persistent and significant increase in the serum CK levels was
459 observed in hDPSC-treated CXMD$_J$ (0 min, 96075 ± 24311 unit/L; 20 min, 95300 ±
460 16835 unit/L) as well as in the untreated CXMD$_J$ (0 min, 76650 ± 46995 unit/L; 20 min,
461 81425 ± 47458 unit/L, p = 0.9277) after exercise. The CXMD$_J$ also showed higher
462 concentration of lactic acid before and after exercise compared to normal dogs. However,
463 the significant change on the levels of lactic acid was not observed in hDPSC-treated
464 CXMD$_J$ (Figure 5D). These findings suggest that IL-10-hDPSCs exert a protective effect
465 against dystrophic damage caused by exercise.

466 Overall, we observed that IL-10-expressing hDPSCs were able to ameliorate
467 the dystrophic phenotype upon systemic repeated administration to dogs with DMD by

the immunomodulation of hDPSCs.

Discussion

To improve the functionality of MSCs as a cell source, we focused on the overexpression of IL-10 based on its anti-apoptotic and anti-inflammatory properties.

Using *in vivo* imaging analysis, the higher survival rate of IL-10-MSCs in the early stage immediately after transplantation is considered to allow long-term cell retention (Figure 1), suggesting stable IL-10 expression enabled the long-term survival and engraftment of MSCs after transplantation. Our findings suggest that during skeletal muscle regeneration, prolonged engraftment of IL-10-expressing $CD271^{+}$MSCs eased the formation of new myofiber-like tissue and the preservation of a functional contractile apparatus, following exposure to the muscle stem cell niche/microenvironment, without any artificial stimulation for myogenic differentiation (Figure 2). Rarely, MSCs differentiate into cells of myogenic lineage in the absence of triggers, such as MyoD [33], 5-azacytidine [34], and Notch I intracellular domain [4]. IL-10 is also considered to play a role in the long-term engraftment, survival, and differentiation of MSCs in muscle tissues.

It was reasoned that IL-10-expressing hDPSCs had enhanced anti-inflammatory and protective effects on damaged tissue, because of the downregulation of MCP-1 and IL-6, and up-regulation of SDF-1 in IL-10-hDPSCs (Figure 3). SDF-1 is crucial factor that supports tissue regeneration, and the roles of SDF-1 in MSC paracrine-mediated tissue repair have been reported [35]. Furthermore, it was also reported that multiple pro-angiogenic factors containing SDF-1, FGF-2, IGF-1, and VEGF-A are enhanced in IL-10-MSC-treated cardiac-muscle [18], suggesting changes in the

surrounding microenvironment.

In the dog model, repeated systemic transplantation hDPSC- and IL-10-expressing hDPSCs were safe and effective as DMD therapeutics, as indicated by blood tests, growth, spontaneous activity, and running function (Figures 3 and 4). Long-term engraftment of hDPSCs was only confirmed in the dystrophic muscles in IL-10-DPSC-treated DMD, which suggests that the engraftment of hDPSCs was enhanced through IL-10 paracrine effects. These facts provide evidence of the accumulation of hDPSCs at the site of inflammation after the systemic administration, similar to MSCs. The functional recovery in the dystrophic skeletal muscle was attributed to the alleviation of the morphological pathologies, such as MRI findings and the histopathological appearance in the hDPSC-, and IL-10-hDPSC-treated $CXMD_J$ (Figure 4). Indeed, both of hDPSC-, and IL-10-hDPSC-treated $CXMD_J$ showed improved limb strength as evidenced by the tetanic force, revealed an improvement in the spontaneous activity and running speed, while no significant difference was observed in the treated $CXMD_J$ on maintaining apparent function. We observed that the IL-10-hDPSC-treated $CXMD_J$ was more stable compared to that in the hDPSC-treated $CXMD_J$, because the increase in serum CK levels after exercise was rapidly stabilized in the IL-10-hDPSC-treated $CXMD_J$ (Figure 5C). These facts suggest that treatment with IL-10-hDPSCs protects from physical damage-induced muscle injury in $CXMD_J$, as opposed to the effect observed in dogs injected with untreated or non-transgenic cells, which is further evidenced by the effects of the modified characteristics of IL-10-hDPSCs involved in SDF-1 and VEGF.

This is the first report of increased cell survival, engraftment, and possible tissue formation of MSCs in muscle tissue by secreting IL-10. In our previous report, myogenic lineage-MSCs were successfully engrafted in muscle tissue [25]. However, a

more efficient transplantation strategy is required for functional improvement of muscle dystrophy. This study evaluates the possibility of improving survival, engraftment, and immune-modulation of MSCs by AAV vector-mediated stable expression of IL-10.

We previously provided evidence that severe phenotypes in IL-10 knockout *mdx* mice, such as increased M1-macrophage infiltration, high inflammatory factor levels, and progressive cardiorespiratory dysfunction, show a predisposition toward inflammation [36]. Glucocorticoids are widely used in patients to interrupt and improve muscle strength during early stages, which may also act directly on muscle fibers by stabilizing the sarcolemma [37, 38], but this is frequently associated with severe side effects. In our strategy, MSCs are appeared to show an inflammatory regulation effects and a protective effect in the dystrophic muscle through the suppress M1-macrophage infiltration by secreting IL-10. In addition, our stable IL-10 expression system is safe, with a low risk of genome insertion owing to the use of an AAV vector. Random integration, off-targeting effects, and poor specificity are associated with the use of other viruses and techniques of genome engineering. IL-10-expressing MSCs are expected to have potential applicability in muscle regeneration and treatment of muscle disease. We previously reported that the overexpression of IL-10 promotes neuroprotection in an experimental acute ischemic stroke model [39]. There is clinical interest in the applicability of IL-10-MSCs in *ex vivo* cell therapy owing to their anti-inflammatory properties and ability to release cytokines into the surrounding environment, which mediates the paracrine effects and thereby modifies the developmental fate of neighboring cells.

Conclusions

methods were developed to enhance MSC survival and improve their therapeutic effects using the anti-inflammatory properties of IL-10 for DMD.

In case of local injection, the IL-10-expressing MSCs could maintain the long-term engraftment status and facilitate associated tissue repair. In case of repeated systemic administration, IL-10-MSCs facilitated the long-term engraftment of the cells in skeletal muscle and also protected muscles with physical damage-induced injury, which improved muscle dysfunction in DMD. We can conclude that the local and systemic administration of IL-10-expressing MSCs may exert beneficial IL-10 paracrine effects, which has potential value in DMD therapeutics.

Availability of data and materials

The datasets used and/or analyzed during the current study are available from the corresponding author on reasonable request.

References

1. Friedenstein AJ, Petrakova KV, Kurolesova AI, and Frolova GP: **Heterotopic of bone marrow. Analysis of precursor cells for osteogenic and hematopoietic tissues.** *Transplantation.* 1968, **6:** 230-247.
2. Bruder SP, Jaiswal N, and Haynesworth SE: **Growth kinetics, self-renewal, and the osteogenic potential of purified human mesenchymal stem cells during extensive subcultivation and following cryopreservation.** *J Cell Biochem.* 1997, **64:** 278-294.
3. Haynesworth SE, Goshima J, Goldberg VM, and Caplan AI: **Characterization of cells with osteogenic potential from human marrow.** *Bone.* 1992, **13:** 81-88.
4. Dezawa M, Ishikawa H, Itokazu Y, Yoshihara T, Hoshino M, Takeda S, Ide C, and Nabeshima Y: **Bone marrow stromal cells generate muscle cells and repair muscle degeneration.** *Science.* 2005, **309:** 314-317.

5. Sun Y, Liu J, Qian F, and Xu Q: **Nitric oxide inhibits T cell adhesion and migration by down-regulation of beta1-integrin expression in immunologically liver-injured mice.** *Int Immunopharmacol.* 2006, **6:** 616-626.
6. Kopen GC, Prockop DJ, and Phinney DG: **Marrow stromal cells migrate throughout forebrain and cerebellum, and they differentiate into astrocytes after injection into neonatal mouse brains.** *Proc Natl Acad Sci U S A.* 1999, **96:** 10711-10716.
7. Ma Y, Xu Y, Xiao Z, Yang W, Zhang C, Song E, Du Y, and Li L: **Reconstruction of chemically burned rat corneal surface by bone marrow-derived human mesenchymal stem cells.** *Stem Cells.* 2006, **24:** 315-321.
8. Nauta AJ, and Fibbe WE: **Immunomodulatory properties of mesenchymal stromal cells.** *Blood.* 2007, **110:** 3499-3506.
9. Rasmusson I, Ringden O, Sundberg B, and Le Blanc K: **Mesenchymal stem cells inhibit the formation of cytotoxic T lymphocytes, but not activated cytotoxic T lymphocytes or natural killer cells.** *Transplantation.* 2003, **76:** 1208-1213.
10. Zappia E, Casazza S, Pedemonte E, Benvenuto F, Bonanni I, Gerdoni E, Giunti D, Ceravolo A, Cazzanti F, Frassoni F, Mancardi G, and Uccelli A: **Mesenchymal stem cells ameliorate experimental autoimmune encephalomyelitis inducing T-cell anergy.** *Blood.* 2005, **106:** 1755-1761.
11. Ichim TE, Alexandrescu DT, Solano F, Lara F, Campion Rde N, Paris E, Woods EJ, Murphy MP, Dasanu CA, Patel AN, Marleau AM, Leal A, and Riordan NH: **Mesenchymal stem cells as anti-inflammatories: implications for treatment of Duchenne muscular dystrophy.** *Cell Immunol.* 2010, **260:** 75-82.
12. Aggarwal S, and Pittenger MF: **Human mesenchymal stem cells modulate allogeneic immune cell responses.** *Blood.* 2005, **105:** 1815-1822.
13. MacDonald KP, Pettit AR, Quinn C, Thomas GJ, and Thomas R: **Resistance of rheumatoid synovial dendritic cells to the immunosuppressive effects of IL-10.** *J Immunol.* 1999, **163:** 5599-5607.
14. Groux H, Bigler M, de Vries JE, and Roncarolo MG: **Inhibitory and stimulatory effects of IL-10 on human CD8+ T cells.** *J Immunol.* 1998, **160:** 3188-3193.
15. Manning E, Pham S, Li S, Vazquez-Padron RI, Mathew J, Ruiz P, and Salgar SK: **Interleukin-10 delivery via mesenchymal stem cells: a novel gene therapy approach to prevent lung ischemia-reperfusion injury.** *Hum Gene Ther.* 2010,

21: 713-727.

16. Min CK, Kim BG, Park G, Cho B, and Oh IH: **IL-10-transduced bone marrow mesenchymal stem cells can attenuate the severity of acute graft-versus-host disease after experimental allogeneic stem cell transplantation.** *Bone Marrow Transplant.* 2007, **39:** 637-645.
17. Peruzzaro ST, Andrews MMM, Al-Gharaibeh A, Pupiec O, Resk M, Story D, Maiti P, Rossignol J, and Dunbar GL: **Transplantation of mesenchymal stem cells genetically engineered to overexpress interleukin-10 promotes alternative inflammatory response in rat model of traumatic brain injury.** *J Neuroinflammation.* 2019, **16:** 2.
18. Meng D, Han S, Jeong IS, and Kim SW: **Interleukin 10-Secreting MSCs via TALEN-Mediated Gene Editing Attenuates Left Ventricular Remodeling after Myocardial Infarction.** *Cell Physiol Biochem.* 2019, **52:** 728-741.
19. Choi JJ, Yoo SA, Park SJ, Kang YJ, Kim WU, Oh IH, and Cho CS: **Mesenchymal stem cells overexpressing interleukin-10 attenuate collagen-induced arthritis in mice.** *Clin Exp Immunol.* 2008, **153:** 269-276.
20. Shimatsu Y, Yoshimura M, Yuasa K, Urasawa N, Tomohiro M, Nakura M, Tanigawa M, Nakamura A, and Takeda S: **Major clinical and histopathological characteristics of canine X-linked muscular dystrophy in Japan, CXMDJ.** *Acta Myol.* 2005, **24:** 145-154.
21. Shimatsu Y, Katagiri K, Furuta T, Nakura M, Tanioka Y, Yuasa K, Tomohiro M, Kornegay JN, Nonaka I, and Takeda S: **Canine X-linked muscular dystrophy in Japan ($CXMD_J$).** *Exp Anim.* 2003, **52:** 93-97.
22. Jo YY, Lee HJ, Kook SY, Choung HW, Park JY, Chung JH, Choung YH, Kim ES, Yang HC, and Choung PH: **Isolation and characterization of postnatal stem cells from human dental tissues.** *Tissue Eng.* 2007, **13:** 767-773.
23. Nito C, Sowa K, Nakajima M, Sakamoto Y, Suda S, Nishiyama Y, Nakamura-Takahashi A, Nitahara-Kasahara Y, Ueda M, Okada T, and Kimura K: **Transplantation of human dental pulp stem cells ameliorates brain damage following acute cerebral ischemia.** *Biomed Pharmacother.* 2018, **108:** 1005-1014.
24. Uchibori R, Okada T, Ito T, Urabe M, Mizukami H, Kume A, and Ozawa K: **Retroviral vector-producing mesenchymal stem cells for targeted suicide**

cancer gene therapy. *J Gene Med.* 2009, **11:** 373-381.

25. Nitahara-Kasahara Y, Hayashita-Kinoh H, Ohshima-Hosoyama S, Okada H, Wada-Maeda M, Nakamura A, Okada T, and Takeda S: **Long-term engraftment of multipotent mesenchymal stromal cells that differentiate to form myogenic cells in dogs with Duchenne muscular dystrophy.** *Mol Ther.* 2012, **20:** 168-177.

26. Nitahara-Kasahara Y, Hayashita-Kinoh H, Chiyo T, Nishiyama A, Okada H, Takeda S, and Okada T: **Dystrophic *mdx* mice develop severe cardiac and respiratory dysfunction following genetic ablation of the anti-inflammatory cytokine IL-10.** *Hum Mol Genet.* 2014, **23:** 3990-4000.

27. Okada T, Nomoto T, Yoshioka T, Nonaka-Sarukawa M, Ito T, Ogura T, Iwata-Okada M, Uchibori R, Shimazaki K, Mizukami H, Kume A, and Ozawa K: **Large-scale production of recombinant viruses by use of a large culture vessel with active gassing.** *Hum Gene Ther.* 2005, **16:** 1212-1218.

28. Okada T, Nonaka-Sarukawa M, Uchibori R, Kinoshita K, Hayashita-Kinoh H, Nitahara-Kasahara Y, Takeda S, and Ozawa K: **Scalable purification of adeno-associated virus serotype 1 (AAV1) and AAV8 vectors, using dual ion-exchange adsorptive membranes.** *Hum Gene Ther.* 2009, **20:** 1013-1021.

29. Hayashita-Kinoh H, Yugeta N, Okada H, Nitahara-Kasahara Y, Chiyo T, Okada T, and Takeda S: **Intra-amniotic rAAV-mediated microdystrophin gene transfer improves canine X-linked muscular dystrophy and may induce immune tolerance.** *Mol Ther.* 2015, **23:** 627-637.

30. Kobayashi M, Nakamura A, Hasegawa D, Fujita M, Orima H, and Takeda S: **Evaluation of dystrophic dog pathology by fat-suppressed T2-weighted imaging.** *Muscle Nerve.* 2009, **40:** 815-826.

31. Kuraoka M, Nitahara-Kasahara Y, Tachimori H, Kato N, Shibasaki H, Shin A, Aoki Y, Kimura E, and Takeda S: **Accelerometric outcomes of motor function related to clinical evaluations and muscle involvement in dystrophic dogs.** *PLoS One.* 2018, **13:** e0208415.

32. Childers MK, Okamura CS, Bogan DJ, Bogan JR, Petroski GF, McDonald K, and Kornegay JN: **Eccentric contraction injury in dystrophic canine muscle.** *Arch Phys Med Rehabil.* 2002, **83:** 1572-1578.

33. Choi J, Costa ML, Mermelstein CS, Chagas C, Holtzer S, and Holtzer H: **MyoD converts primary dermal fibroblasts, chondroblasts, smooth muscle, and**

retinal pigmented epithelial cells into striated mononucleated myoblasts and multinucleated myotubes. *Proc Natl Acad Sci U S A.* 1990, **87:** 7988-7992.

34. Balana B, Nicoletti C, Zahanich I, Graf EM, Christ T, Boxberger S, and Ravens U: **5-Azacytidine induces changes in electrophysiological properties of human mesenchymal stem cells.** *Cell Res.* 2006, **16:** 949-960.

35. Luo Q, Zhang B, Kuang D, and Song G: **Role of Stromal-Derived Factor-1 in Mesenchymal Stem Cell Paracrine-Mediated Tissue Repair.** *Curr Stem Cell Res Ther.* 2016, **11:** 585-592.

36. Nitahara-Kasahara Y, Takeda S, and Okada T: **Inflammatory predisposition predicts disease phenotypes in muscular dystrophy.** *Inflamm Regen.* 2016, **36:** 14.

37. Jacobs SC, Bootsma AL, Willems PW, Bar PR, and Wokke JH: **Prednisone can protect against exercise-induced muscle damage.** *J Neurol.* 1996, **243:** 410-416.

38. Serra F, Quarta M, Canato M, Toniolo L, De Arcangelis V, Trotta A, Spath L, Monaco L, Reggiani C, and Naro F: **Inflammation in muscular dystrophy and the beneficial effects of non-steroidal anti-inflammatory drugs.** *Muscle Nerve.* 2012, **46:** 773-784.

39. Nakajima M, Nito C, Sowa K, Suda S, Nishiyama Y, Nakamura-Takahashi A, Nitahara-Kasahara Y, Imagawa K, Hirato T, Ueda M, Kimura K, and Okada T: **Mesenchymal Stem Cells Overexpressing Interleukin-10 Promote Neuroprotection in Experimental Acute Ischemic Stroke.** *Mol Ther Methods Clin Dev.* 2017, **6:** 102-111.

Acknowledgments

The authors express their gratitude to Akihiko Umezawa, Akinori Nakamura, Tetsuya Nagata, Masanori Kobayashi, Yuko Shimizu-Motohashi, Jun Tanihata, Michihiro Imamura, and Kazuhiro Yamamoto for their technical advice, support, and helpful discussions; Tomoko Chiyo, Chiaki Masuda, Kazue Kinoshita, Ryoko Nakagawa, and

Rie Ogawa for technical assistance; Hideki Kita, Shinichi Ichikawa, Yumiko Yahata-Kobayashi, Aya Kuriyama, Akane Hanaoka-Hayashi, Namiko Ogawa, and other staff members of JAC Co. for caring for the dogs (General Animal Research Facility, NCNP). We are thankful to JCR Pharmaceuticals Co., Ltd for their generous contribution of the DPSCs and MSCs. We also thank Posadas Herrera Guillermo for checking the quality of English in the manuscript.

Funding

This work was supported by a research grant from JCR Pharmaceuticals Co., Ltd., Health Sciences Research Grants for Research on Human Genome and Gene Therapy from the Ministry of Health, Labor and Welfare of Japan, and a Grant-in-Aid for Scientific Research from the Ministry of Education, Culture, Sports, Science and Technology (grant number: 22390284, 22-40134).

Contributions

Y. N-K. and T. O. conceived and planned the experiments. Y. N-K. and M.K. performed the experiments, derived the models, and analyzed the data. H. H-K. Y.O. and M.K. contributed to sample preparation and assisted with experiments involving animal models. Y. N-K. wrote the manuscript in consultation, and T.O. and S.T. helped supervise the project. T.O. supervised the project.

Ethics approval and consent to participate

Animal experiments using MSCs were conducted in accordance with the protocol approved by the Institutional Animal Care and Use Committee of Nippon Medical School (27-199) and National Center of Neurology and Psychiatry (NCNP) Animal Ethics Committees (2012011, 2015004, and 19–30-06).

Consent for publication

Not applicable.

Conflicts of Interest

Y. N-K., T. O. and S.T. have patent applications related to MSCs expressing IL-10. H. H-K., Y. N-K. and T. O. were members of the Division of Cell and Gene Therapy, Nippon Medical School, which is an endowment department, supported with a grant from JCR Pharmaceuticals Co., Ltd and Kaneka corporation.

Supplementary Information

Additional file 1. *In vivo* bioluminescence imaging for the detection of injected MSCs

Additional file 2. Enhanced engraftment of IL-10-expressing MSCs

Additional file 3. IL-10 expression in IL-10-MSC-treated muscle

Additional file 4. Quantitative monitoring data of surviving MSCs

Additional file 5. Serum chemistry data from the hDPSC-treated $CXMD_J$ model

Additional file 6. Monitoring data of thigh circumference in the $CXMD_J$ model

Additional file 7. Estimated isometric tetanic force in hDPSC-treated $CXMD_J$

Additional file 8. 15-meter running speed of hDPSC-treated $CXMD_J$

Additional file 9. Supplemental Methods and Table 1. Running speed (15-m) of dogs at 12 to 44 months of age

Table I. Summary of transplantation experiments

Dog ID	Sex	Age[a]	BW[b]	Cell	Cell numbers	Interval	Injection numbers	Route
4502MN	M	51	11.3	IL-10-CD271$^+$MSCs, MyoD-CD271$^+$MSCs	2.5 $\times 10^7$ cells	-	1	i.m.[c]
5601MN	M	40	11.2	IL-10-CD271$^+$MSCs, MyoD-CD271$^+$MSCs	4.0-10.0$\times 10^6$ cells	-	2	i.m.[c]
14103MN	M	3	5.0	-	-	-	-	-
14102MA	M	3	3.3	-	-	-	-	-
14105MA	M	3	3.4	hDPSCs	4.0 x10^6 cells/kg	2 weeks	9	i,v.[d]
14108MA	M	3	3.5	IL-10-hDPSCs	4.0 x10^6 cells/kg	2 weeks	9	i,v.[d]

M, male; [a]Age at injection (months); [b]BW, body weight at first injection (kg); [c]i.m, intramuscular injection; [d]i.v., intravenous injection

747 **Figure Legends**

748 **Figure 1. Extended engraftment of IL-10-expressing MSCs**

749 Luciferase-expressing MSCs were transduced using control AAV1/enhanced green
750 fluorescence protein (GFP) or the AAV1/IL-10 vector. (A) Quantitative measurement of
751 IL-10 expression in the MSC medium was performed using ELISA at 7 days after
752 transduction. Data are presented as mean ± SD and statistical differences between eGFP-
753 MSC-treated mice vs. IL-10-MSC-treated mice, $^{****}P < 0.0001$, *t*-test are indicated.
754 MSCs expressing GFP or IL-10 were injected into the right or left site hind-limb muscle
755 (IL-10(-) or IL-10(+)) of NOD/SCID mice. (B) IL-6 expression in the hind-limb muscle
756 (IL-10(-) or IL-10(+)) of the mice at 4 and 9 days after transplantation was analyzed using
757 real-time PCR. (C) *In vivo* bioluminescence imaging of the MSC-treated mice revealed
758 the appearance of luciferase signals between 3 and 67 days after intramuscular injection.
759 (D) Monitoring of the quantitative luciferase counts at the GFP- or IL-10-MSCs-injected
760 site from imaging analysis conducted between 3 and 67 days after treatment (n = 6–3).

761

762 **Figure 2. Successful long-term engraftment of canine IL-10-MSCs in the skeletal**
763 **muscles of dogs**

764 (A) Transplantation schedule. Canine $CD271^+$MSCs expressing luciferase (Luc-
765 $CD271^+$MSCs) were transduced with AAV1/IL-10 in the cardiotoxin-pretreated tibialis
766 anterior (TA) muscle of the recipient dog. (B) Immunohistochemical analysis by
767 horseradish peroxidase (HRP)-diaminobenzidene (DAB)-labeled observation of the TA
768 muscle derived from IL-10- Luc-$CD271^+$ MSC-treated muscle (4502MN) at 4 weeks after
769 injection. Dotted line circles (blue) and arrows indicate accumulation of luciferase-
770 immunopositive MSCs. Scale bar, 100 μm. (C) Immunofluorescence analysis of the TA

muscle derived from an IL-10-Luc-CD271^{+}MSC-treated dog (5601MN) 8 weeks after injection using antibodies specific for luciferase (red), dystrophin (green) and nuclear stain 4',6'-diamidino-2-phenylindole (DAPI, blue). The square frames on the right side of the images represent a greater magnification. Arrow head, luciferase-positive myofiber; Bar = 200 μm. (D) Luciferase assays to determine the cell number in the IL-10-Luc-CD271^{+}MSC- (IL-10-MSC) or MyoD-Luc-CD271^{+}MSC (MyoD-MSC)-treated TA muscle lysate. (E) Quantitative measurement of IL-10 levels in the IL-10-MSC- or MyoD-MSC-treated TA muscle lysate (mg protein) using ELISA. Data are presented as mean ± SD, and statistical differences between MyoD-MSC- and IL-10-MSC-treated TA muscle are indicated, $^{*}P < 0.05$.

Figure 3. Safe systemic treatment of IL-10-expressing hDPSCs in the CXMD$_J$ model and successful long-term engraftment

(A) Transplantation schedule. (B) Quantitative measurement of IL-10 expression in 2-day culture medium and in the hDPSC lysate (100 mg) using ELISA. Data are presented as mean ± SD and statistical differences between hDPSCs vs. IL-10-hDPSCs are indicated ($^{****}P < 0.001$, n = 3). (C) Cytokine and chemokine expression in 2-day culture medium of hDPSCs and IL-10-hDPSCs analyzed using the Proteome ProfilerTM Array. Changes in the expression levels of monocyte chemotactic protein-1 (MCP-1), IL-6, and stromal-derived factor-1 (SDF-1/CXCL12), compared to the positive control (PC) signals or negative control (NC). Signal intensity in the regions of interest (ROIs) quantified using array images (upper panels) and representative data (graph) are presented. ND, not detected. (D) Growth curve of untreated CXMD$_J$ (control DMD; 14102MA), hDPSC-, and IL-10-hDPSC-treated CXMD$_J$ (hDPSC-DMD, 14105MA; IL-10-hDPSC-DMD,

14108MA) dogs. Data are presented as mean ± SD and statistical differences between control DMD vs. IL-10-hDPSC-DMD ($^{****}P < 0.001$), hDPSC-DMD vs. IL-10-hDPSC-DMD ($^{\#\#\#\#}P < 0.001$) are indicated; two-way ANOVA. (E) Serum levels of IL-10 at 6, 24, and 48 h, and 7 days after transplantation, quantified using ELISA. Data are presented as mean ± SD and statistical differences between control DMD vs. IL-10-hDPSC-DMD ($^{*}P < 0.05$, $^{**}P < 0.01$, $^{****}P < 0.0001$), hDPSC-DMD vs. IL-10-hDPSC-DMD ($^{\#}P < 0.05$, $^{\#\#\#\#}P < 0.0001$) are indicated; ns, not significant, two-way ANOVA.

Figure 4. Improvement in the hDPSC-treated CXMD$_J$ model observed by histological examination

(A) Cross-sectional magnetic resonance images (MRI) in the lower leg muscles of normal dogs, untreated CXMD$_J$ (control DMD), hDPSC-treated (hDPSC-DMD), and IL-10-hDPSCs-treated CXMD$_J$ (IL-10-hDPSCs-DMD). Muscle necrosis and inflammation based on the sequence of T2-weighted imaging of the lower legs for each dog were comparable (R, right side; L, left side, left/right asymmetry). (B) The averaged signal-to-noise ratios (Ave SNR) were calculated in the regions of interest (ROIs) from all muscles (n=14) derived from each hind-limb of 2-month-old (before transplantation) and 7-month-old dogs (after transplantation). Data are presented as mean ± SD, and statistical differences between normal vs. control DMD ($^{****}P < 0.0001$), hDPSC-DMD vs. IL-10-hDPSC-DMD ($^{\#\#}P = 0.008$) are indicated; ns, not significant, two-way ANOVA. (C) Hematoxylin and eosin (H&E) staining of the gastrocnemius lateral head (GL) and extensor digitorum longus (EDL) muscle from 1-year-old control DMD, hDPSC-DMD, and IL-10-hDPSC-DMD dogs. Scale bar, 100 μm.

Figure 5. Improved locomotor activity in CXMD$_J$ treated with IL-10-expressing MSCs

(A) Day-time behavioral activity of normal (left graph), untreated CXMD$_J$ (control DMD), hDPSC-treated CXMD$_J$ (hDPSC-DMD), and IL-10-hDPSC-treated CXMD$_J$ (IL-10-hDPSC-DMD) in home cage at 3, 6, and 12 months presented as mean counts activity (average of value for 5 days). Statistical differences between control DMD vs. hDPSC-DMD or IL-10-hDPSC-DMD dog groups ($^{\#}P < 0.05$, $^{\#\#}P < 0.01$, $^{\#\#\#}P < 0.001$, $^{\#\#\#\#}P < 0.0001$) are indicated; ns, not significant, two-way ANOVA. (B) 15-meter running speed of normal, control DMD, hDPSC-DMD, and IL-10-hDPSC-DMD dogs at 12 months. The mean value was the average value of four measurements from each group. Statistical differences between normal vs. DMD ($^{*}P < 0.05$, $^{**}P < 0.01$, and $^{****}P < 0.0001$), control DMD vs. hDPSC-DMD, or IL-10-hDPSC-DMD ($^{\#}P < 0.05$, $^{\#\#}P < 0.01$, $^{\#\#\#}P < 0.001$) are indicated; ns, not significant, one-way ANOVA. (C) Serum creatine kinase (CK) levels and (D) serum levels of lactic acid of each group before, 0, and 20 min after running exercise, which were four 4 times greater than those after 15-meter running, as measured by ELISA. Statistical differences between normal vs. DMD ($^{*}P < 0.05$, $^{**}P < 0.01$), control DMD vs. IL-10-hDPSC-DMD ($^{\#}P < 0.05$) are indicated; two-way ANOVA. n = 4 for each group. All data are presented as the mean ± SD.

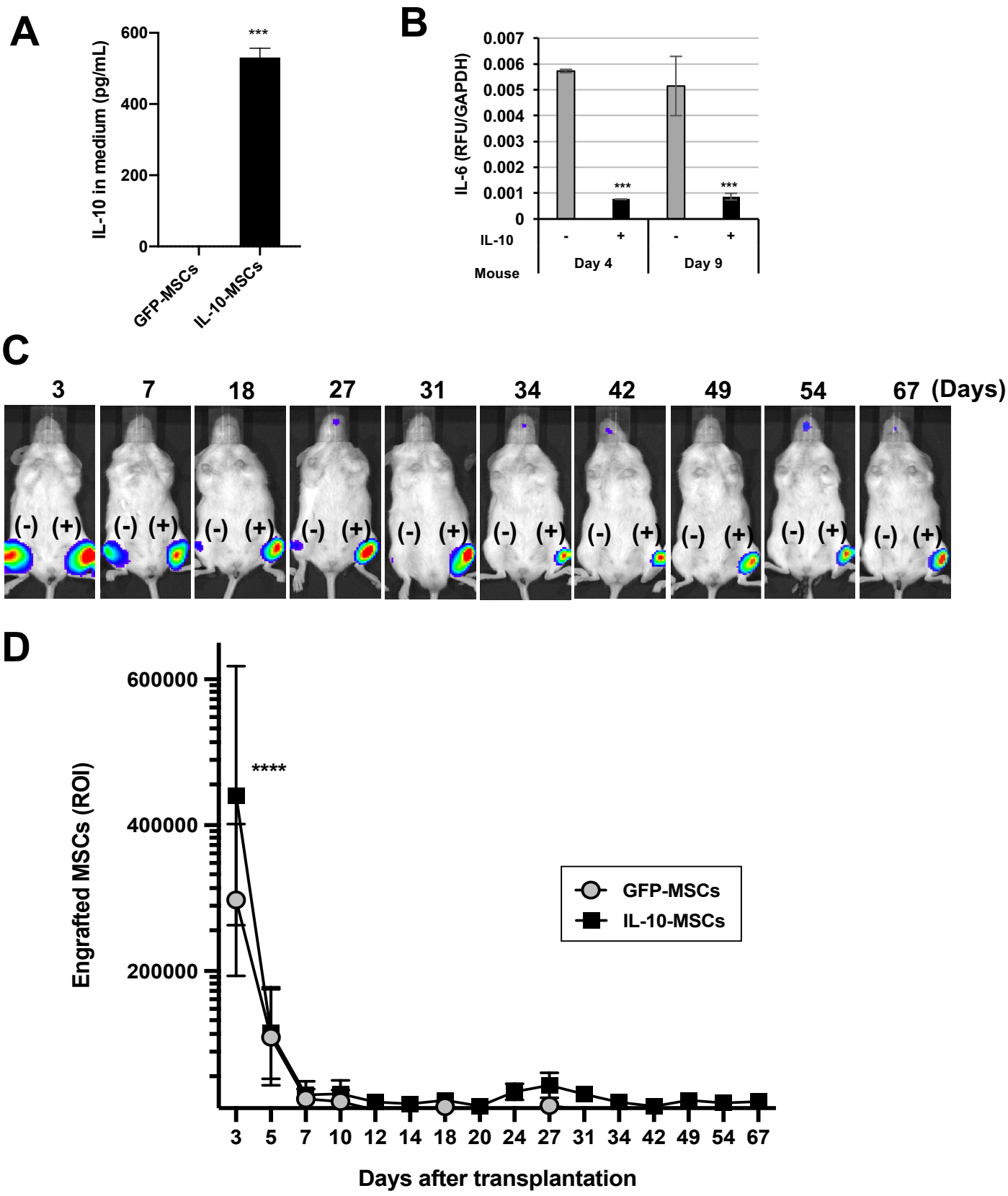
A
IL-10 in medium (pg/mL)
600
400
200
0
***
GFP-MSCs
IL-10-MSCs
B
IL-6 (RFU/GAPDH)
0.007
0.006
0.005
0.004
0.003
0.002
0.001
0
***
***
IL-10
-
+
-
+
Mouse
Day 4
Day 9
C
3
7
18
27
31
34
42
49
54
67
(Days)
(-) (+)
D
Engrafted MSCs (ROI)
600000
400000
200000
****
GFP-MSCs
IL-10-MSCs
3 5 7 10 12 14 18 20 24 27 31 34 42 49 54 67
Days after transplantation

Figure. 1

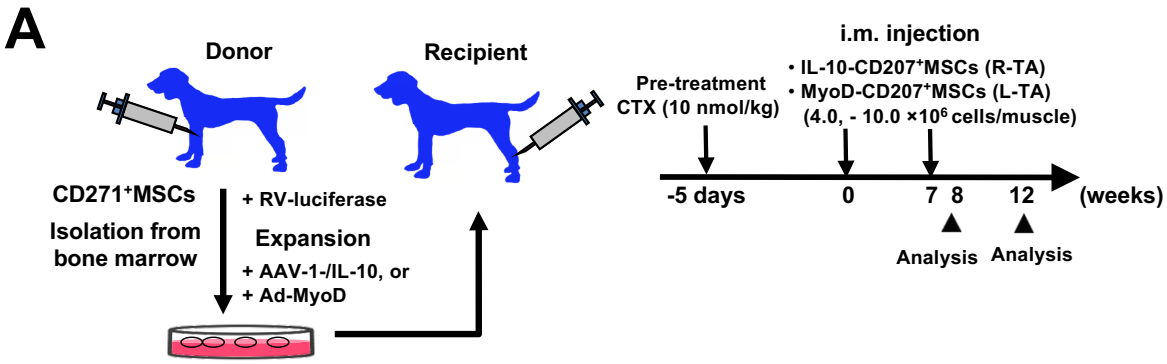
A
Donor
Recipient
CD271+MSCs
Isolation from
bone marrow
+ RV-luciferase
Expansion
+ AAV-1-/IL-10, or
+ Ad-MyoD
i.m. injection
• IL-10-CD207+MSCs (R-TA)
• MyoD-CD207+MSCs (L-TA)
(4.0, - 10.0 ×10^6 cells/muscle)
Pre-treatment
CTX (10 nmol/kg)
-5 days
0
7
8
12
(weeks)
Analysis
Analysis

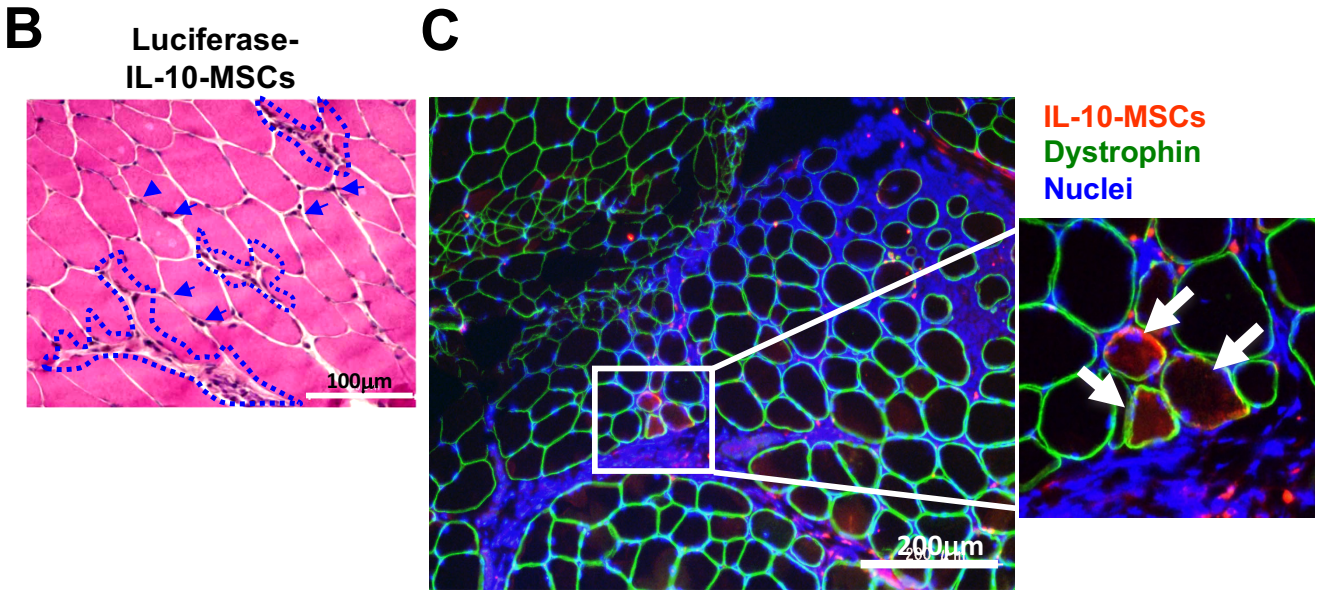
B
Luciferase-
IL-10-MSCs
100μm
C
IL-10-MSCs
Dystrophin
Nuclei
200μm

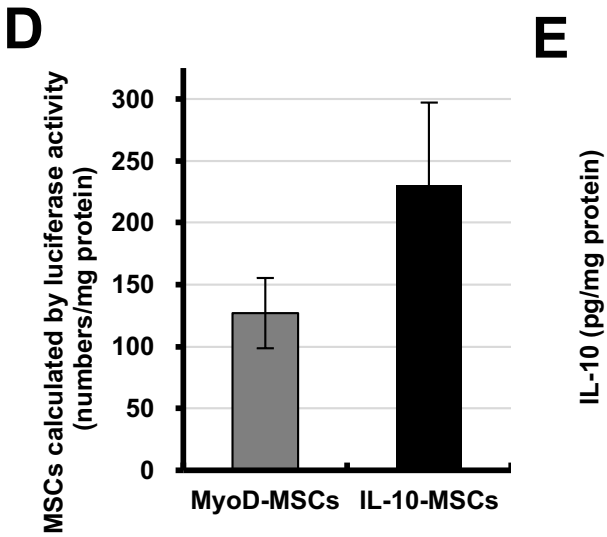
D
MSCs calculated by luciferase activity
(numbers/mg protein)
300
250
200
150
100
50
0
MyoD-MSCs
IL-10-MSCs

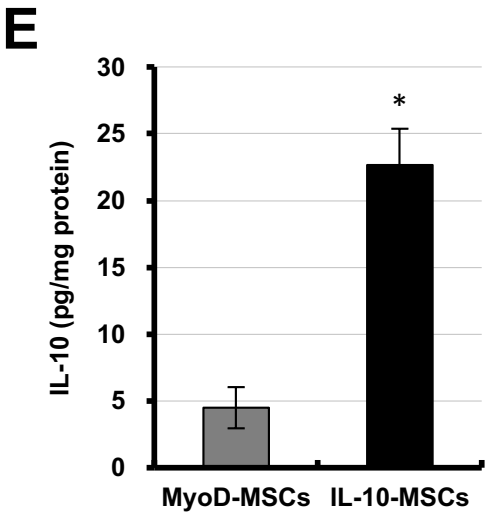
E
IL-10 (pg/mg protein)
30
25
20
15
10
5
0
*
MyoD-MSCs
IL-10-MSCs

Figure. 2

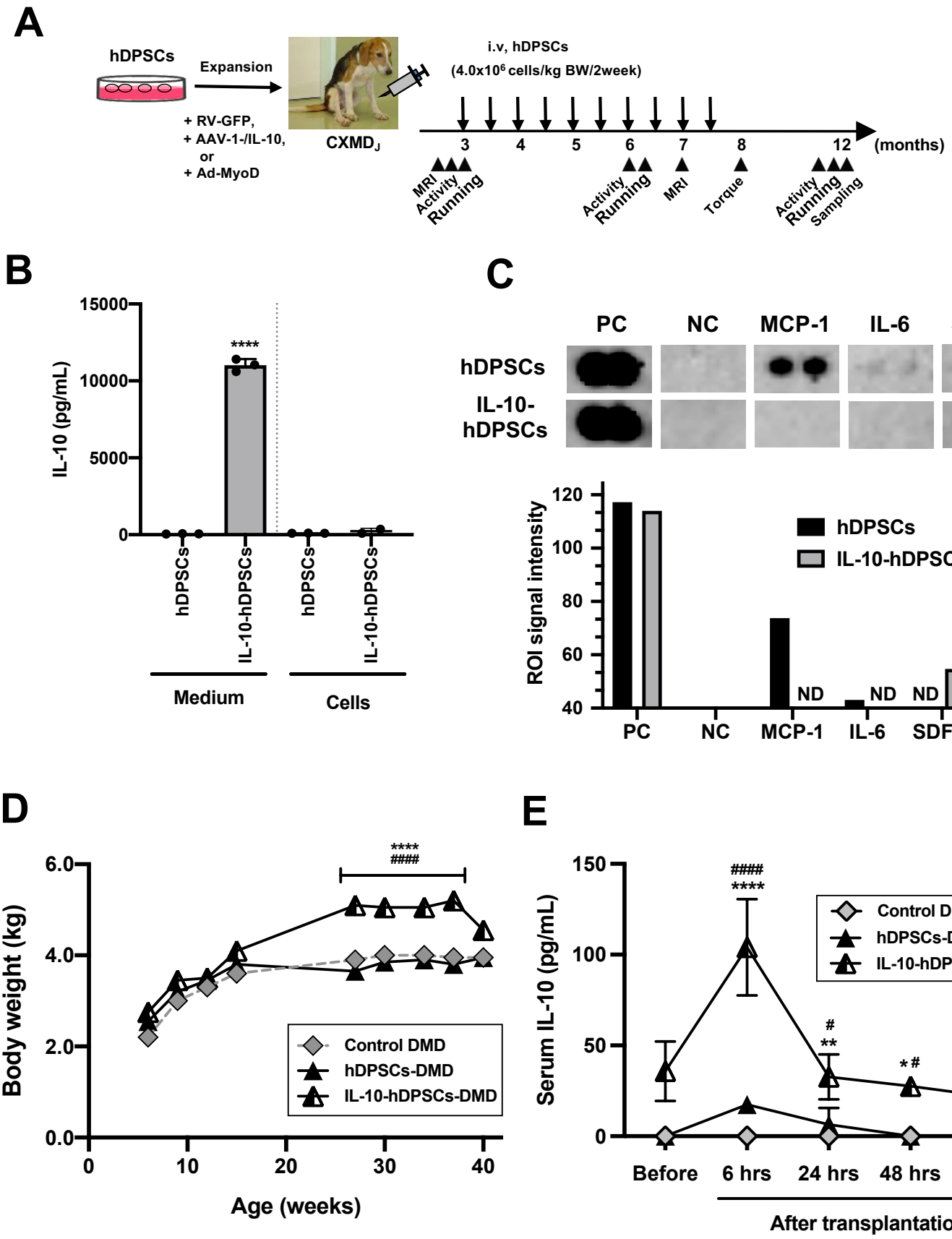
A
hDPSCs
Expansion
+ RV-GFP,
+ AAV-1-/IL-10,
or
+ Ad-MyoD
CXMD$_J$
i.v, hDPSCs
(4.0x10^6 cells/kg BW/2week)
3
4
5
6
7
8
12
(months)
MRI
Activity
Running
Activity
Running
MRI
Torque
Activity
Running
Sampling
B
IL-10 (pg/mL)
15000
10000
5000
0
****
hDPSCs
IL-10-hDPSCs
hDPSCs
IL-10-hDPSCs
Medium
Cells
C
PC
NC
MCP-1
IL-6
SDF-1
hDPSCs
IL-10-hDPSCs
ROI signal intensity
120
100
80
60
40
hDPSCs
IL-10-hDPSCs
ND
ND
ND
PC
NC
MCP-1
IL-6
SDF-1
D
Body weight (kg)
6.0
4.0
2.0
0.0
****
####
Control DMD
hDPSCs-DMD
IL-10-hDPSCs-DMD
0
10
20
30
40
Age (weeks)
E
Serum IL-10 (pg/mL)
150
100
50
0
####
****
#
**
*#
ns
Control DMD
hDPSCs-DMD
IL-10-hDPSCs-DMD
Before
6 hrs
24 hrs
48 hrs
7 days
After transplantation

Figure. 3

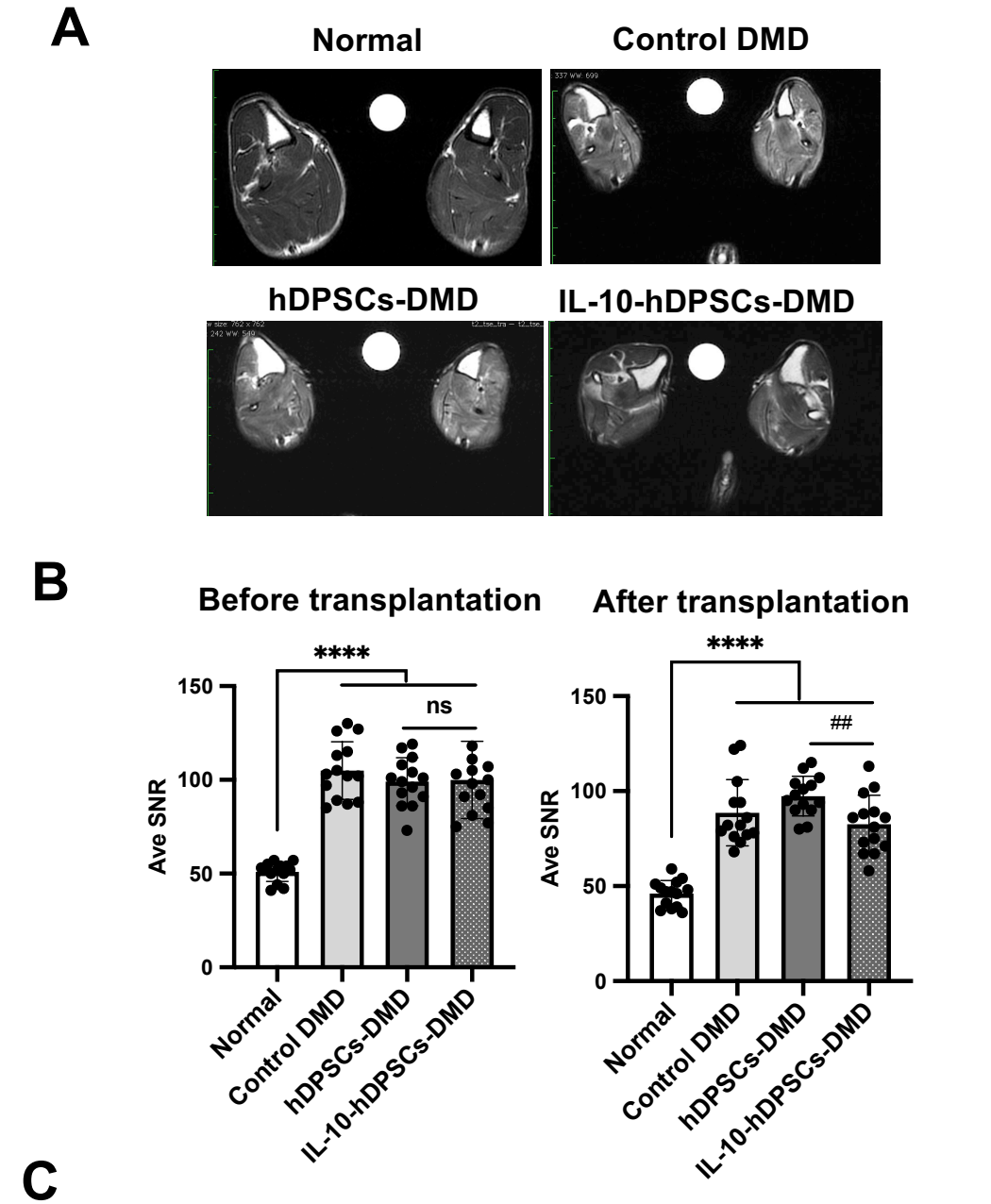
A
Normal
Control DMD
hDPSCs-DMD
IL-10-hDPSCs-DMD
B
Before transplantation
After transplantation
****
ns
##
Ave SNR
150
100
50
0
Normal
Control DMD
hDPSCs-DMD
IL-10-hDPSCs-DMD
C
Control DMD
hDPSCs-DMD
IL-10-hDPSCs-DMD
GL
EDL
100μm

Figure. 4

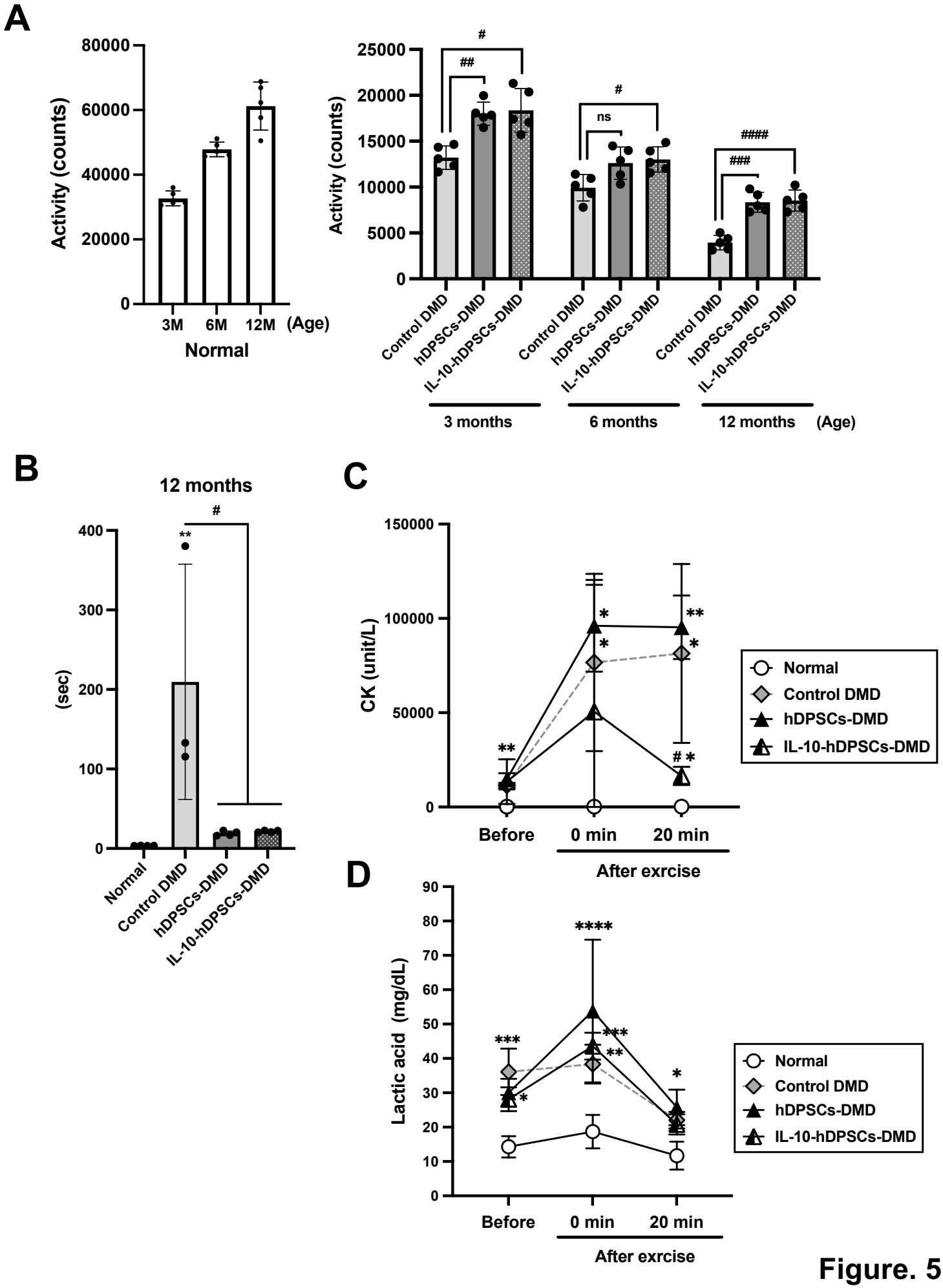
A
Activity (counts)
80000
60000
40000
20000
0
3M
6M
12M
(Age)
Normal
Activity (counts)
25000
20000
15000
10000
5000
0
#
##
ns
#
####
###
Control DMD
hDPSCs-DMD
IL-10-hDPSCs-DMD
3 months
6 months
12 months
(Age)
B
12 months
(sec)
400
300
200
100
0
**
#
Normal
Control DMD
hDPSCs-DMD
IL-10-hDPSCs-DMD
C
CK (unit/L)
150000
100000
50000
0
Before
0 min
20 min
After exrcise
Normal
Control DMD
hDPSCs-DMD
IL-10-hDPSCs-DMD
D
Lactic acid (mg/dL)
90
80
70
60
50
40
30
20
10
0
****
***
Before
0 min
20 min
After exrcise
Normal
Control DMD
hDPSCs-DMD
IL-10-hDPSCs-DMD

Figure. 5